

# The magnetism of the $t - t'$ Hubbard model

B. Valenzuela $\S^1$ , M.A.H. Vozmediano $\dagger^2$ , and F. Guinea $\S^3$

$\S$ *Instituto de Ciencia de Materiales, CSIC  
Cantoblanco, 28049 Madrid, Spain.*

$\dagger$ *Departamento de Matemáticas, Universidad Carlos III de Madrid  
Avda. de la Universidad 30, 28913 Leganés (Madrid), Spain.*

## Abstract

The magnetic properties of the  $t - t'$  Hubbard model in the two dimensional square lattice are studied within an unrestricted Hartree Fock approximation in real space. The interplay between antiferromagnetism, ferromagnetism, phase separation and inhomogeneous magnetic textures is studied. It is shown that, at sufficiently large values of  $t'/t$ , a rich fenomenology is to be expected between the antiferromagnetic phase at half filling and the ferromagnetic phase at lower fillings.

PACS numbers: 75.10.Jm, 75.10.Lp, 75.30.Ds.

---

<sup>1</sup>e-mail: belen@jambo.icmm.csic.es

<sup>2</sup>e-mail: vozmediano@pinar1.csic.es

<sup>3</sup>e-mail: paco.guinea@uam.es

# 1 Introduction

The single band Hubbard model is widely accepted as the simplest starting point of a microscopic description of correlated electron systems [1]. More recently it has been realized that inclusion of a  $t'$  coupling [2] can fit the phenomenology of some cuprates. Recent photoemission experiments seem to provide Fermi surfaces compatible with the dispersion relation of the model at moderate values of  $t'$  and densities [3], while it has been argued that it can fit some features of ruthenium compounds [4] at higher values of  $t'$  and the doping.

The study of inhomogeneous charge and spin phases in the Hubbard model has been a subject of interest since the discovery of the high- $T_c$  compounds as it was seen that they have a very inhomogeneous electronic structure at least in the underdoped regime. However most of the work was done before the importance of  $t'$  was realized [5, 6, 7, 8]. A sufficiently large value of the ratio  $t'/t$ , compatible with the values suggested for the cuprates ( $t'/t \sim -0.3$ ), leads to a significant change in the magnetic properties of the model, as a ferromagnetic phase appears at low doping. This phase has been found by numerical and analytical methods [9, 10, 11], and it is a very robust feature of the model.

The purpose of this work is to study the influence of  $t'$  on the magnetism of the Hubbard model at moderate values of  $U$  and density. We will make use of an unrestricted Hartree-Fock approach in real space what allows us to visualize the charge and spin configurations. We believe that the method is well suited for the present purposes as: i) it gives a reasonable description of the Néel state, with a consistent description of the charge gap and spin waves, when supplemented with the RPA. ii) It becomes exact if the ground state of the model is a fully polarized ferromagnet, as, in this case, the interaction plays no role. A fully polarized ground state is, indeed, compatible with the available Montecarlo[9] and t-matrix calculations[10]. iii) It is a variational technique, and it should give a reasonable approximation to the ground state energy. This is the only ingredient required in analyzing the issue of phase separation. iv) It describes the doped antiferromagnet, for  $t' = 0$  as a dilute gas of spin polarons. The properties of such a system are consistent with other numerical calculations of the same model [12, 13].

On the other hand, the method used here does not allow us to treat possible superconducting instabilities of the model, which have been shown to be present, at least in weak coupling approaches [11]. The study of these phases requires extensions of the present approach, and will be reported elsewhere.

The main new feature introduced by a finite  $t'$ , using simple concepts in condensed matter physics, is the destruction the perfect nesting of the Fermi surface at half filling, and the existence of a second interesting filling factor, at which the Fermi surface includes the saddle points in the dispersion relations. At this filling, the density of states at the Fermi level becomes infinite, and the metallic phase becomes unstable, even for infinitesimal values of the interaction. For sufficiently large values of  $t'/t$ , the leading instability at this filling is towards a ferromagnetic state.

In the following section, we present the model and the method. Then, we discuss the results. As the system shows a rich variety of behaviors, we have classified the different regimes into an antiferromagnetic region, dominated by short range antiferromagnetic correlations, a ferromagnetic one, and an intermediate situation, where the method suggest the existence of phase separation. The last section presents the main conclusions of our work.

## 2 The model and the method

The t-t' Hubbard model is defined in the two dimensional squared lattice by the hamiltonian

$$H = -t \sum_{\langle i,j \rangle, s} c_{i,s}^\dagger c_{j,s} - t' \sum_{\langle\langle i,j \rangle\rangle, s} c_{i,s}^\dagger c_{j,s} + U \sum_i n_{i,\uparrow} n_{i,\downarrow} , \quad (1)$$

with the dispersion relation

$$\varepsilon(\mathbf{k}) = 2t [\cos(k_x a) + \cos(k_y a)] + 4t' \cos(k_x a) \cos(k_y a) .$$

We have adopted the convention widely used to describe the phenomenology of some hole-doped cuprates [2],  $t > 0$ ,  $t' < 0$ ,  $2t'/t < 1$ . With this choice of parameters the bandwidth is  $W = 8t$  and the Van Hove singularity is approached by doping the half-filled system with holes. Throughout this study we will fix the value of  $t = 1$  so that energies will be expressed in units of  $t$ . Unless otherwise stated, we will work in a  $12 \times 12$  lattice with periodic boundary conditions. We have chosen the  $12 \times 12$  lattice because it is the minimal size for which finite size effects are almost irrelevant [6, 15, 16].

The unrestricted Hartree-Fock approximation minimizes the expectation value of the hamiltonian (1) in the space of Slater determinants. These are ground states of a single particle many-body system in a potential defined by the electron occupancy of each site. This potential is determined selfconsistently

$$H = - \sum_{i,j,s} t_{ij} c_{i,s}^\dagger c_{j,s} - \sum_{i,s,s'} \frac{U}{2} \vec{m}_i c_{i,s}^\dagger \vec{\sigma}_{s,s'} c_{i,s'} + \sum_i \frac{U}{2} q_i (n_{i\uparrow} + n_{i\downarrow}) + c.c. ,$$

(where  $t_{i,j}$  denotes next, t, and next-nearest, t', neighbors), and the self-consistency conditions are

$$\vec{m}_i = \sum_{s,s'} \langle c_{i,s}^\dagger \vec{\sigma}_{s,s'} c_{i,s'} \rangle , \quad q_i = \langle n_{i\uparrow} + n_{i\downarrow} - 1 \rangle ,$$

where  $\vec{\sigma}$  are the Pauli matrices.

We have established a very restrictive criterium for the convergence of a solution. The iteration ends when the effective potential of the hamiltonian and the one deduced from the solution are equal up to  $E < 10^{-7}$ . When different configurations converge for a given value of the parameters, their relative stability is found by comparing their total energies.

### 3 The results

The results in this work are summarized in fig.1 which represents the energy of the ground state configurations versus doping from  $x = 0$  to  $x = 0.34$  (where  $x$  is the rate of total number of electrons over the total number of sites) for the representative values  $t' = 0.3$  and  $U = 8$ . As, in most cases, a variety of selfconsistent solutions can be found, we have tried to avoid an initial bias by starting with random spin and charge configurations. Once the system has evolved to a stable final configuration, this has been used as initial condition for the nearby dopings. Hence, most of the configurations discussed in the text are robust in the sense that they have not been forced by a choice of initial conditions and hence are stable under small changes of the initial values. Exceptions are the diagonal commensurate domain walls and the stripes. These configurations were set as initial conditions and found to be self-consistent. Even if there are many possible solutions, the system cannot be “forced ” to converge to a given solution by appropriately choosing the initial conditions. In particular homogeneous solutions, such as a pure AF solution, do not converge near half filling, as will be discussed later. Fig. 2 and fig. 3 show a comparison of the energies of different configurations converging in the same range of dopings. Fig. 1 shows only minimal energy configurations. Once a configuration converges, we have checked its stability under changes in  $U$  and  $t'$ .

The most remarkable feature of fig. 1 is the smooth transition from insulating antiferromagnetism to metallic ferromagnetism. The antiferromagnetic region extends in a range of hole doping from  $x = 0$  to  $x = 0.125$  and the ferromagnetic region from  $x = 0.125$  to  $x = 0.34$ . In the antiferromagnetic region the predominant configurations are fully polarized antiferromagnetism (AF), polarons (POL), diagonal commensurate domain-walls(dcDW), and noncollinear solutions ( $S_x$ ). In the ferromagnetic region the phases are ferromagnetic domains (fm DOM), ferromagnetic non collinear solutions (fm SDW) and the fully polarized state or Nagaoka configuration (Ng).

Most of the AF configurations are known as solutions of the Hubbard model with  $t' = 0$  [5, 6, 7, 8, 17, 18]. We will here comment on the changes induced by  $t'$ . The FM configurations are totally new and due to the presence of  $t'$ , as well as the zone of coexistence of both magnetic orderings. In addition, we have also analyzed in detail some striped configurations, due to their possible experimental relevance.

In what follows we analyze the antiferromagnetic and ferromagnetic regions and discuss the possibility of phase separation.

#### 3.1 The antiferromagnetic region

The study of the motion of a few holes in an antiferromagnetic background has been one of the main subjects in the literature related to the cuprates as these are doped AF insulators. The region of the Hubbard model at and close to half filling is also the area where the metal-insulator transition [19] occurs, and where the well-established spin polarons or spin bags [20] coexist with domain walls and, possibly, striped configurations. The diagonal hopping  $t'$  has a strong influence over this region as it destroys the perfect nesting of the

Hubbard model at half filling and the particle-hole symmetry which leads to AFM order in weak coupling approaches [14, 21].

The AF region is formed by fully polarized antiferromagnetism, polarons, diagonal commensurate domain-walls and non collinear solutions. We also have found stripes as excited states. The configurations and the density of states are shown in fig. 4, fig. 5, fig. 6 and fig.7. We will give a brief discussion of these configurations.

### Antiferromagnetism

For the reference values of  $U = 8$  and  $t' = 0.3$  fully polarized antiferromagnetism (AF) is the lowest energy configuration only at half filling. For the range of dopings  $0.007 \leq x \leq 0.027$ , ( $1 \leq h \leq 4$ , where  $h$  denotes the number of holes), AF converges but POL are energetically more favourable. Above four holes a purely AF initial configuration evolves to polarons.

AF is the minimal energy configuration for lower values of  $U$  in a wider range of dopings. For example for  $U = 4$  and  $t' = 0.3$  AF is the lowest energy configuration in the range  $0 \leq x \leq 0.03$ . This result is almost insensitive to changes in  $t'$ .

We can conclude then that in the presence of  $t'$ , the homogeneous fully polarized antiferromagnetic configuration (Nèel state) is not the dominant solution near half filling. This result is to be contrasted with what happens with electron doping where AF dominates a larger region of the doping space. The reason for this asymmetry will become clear in the discussion of the polaronic configuration following. For  $t' \neq 0$  inhomogeneous solutions are clearly energetically more favourable.

### Polarons

Magnetic polarons have been discussed at length in the literature [20, 8, 22]. For  $t' = 0$  the magnetization points along the same direction everywhere in the cluster and the extra charge is localized in regions that can be of either cigar or diamond shape. These regions defined a core where the magnetization is reduced.

In the present case,  $t' \neq 0$ , this picture changes substantially. The two Hubbard bands in the Nèel state are no longer equivalent, with bandwidths given, approximately, by  $8|t'| \pm 4t^2/U$ . Polarons are found at the edges of the narrower band at all values of  $t'$ . This situation corresponds to hole doping for our choice of sign of  $t'$  ( $t'/t < 0$ ). The doping of the wider electron band leads usually to stable homogeneous metallic AF solutions, where the extra carriers are delocalized throughout the lattice. We have found polarons in the electron region only when  $U$  is big ( $U > 6$ ) and  $t'$  small ( $t' < 0.15$ ). On the other hand, the localization of the polarons induced by hole doping increases with increasing  $|t'/t|$ . This reflects the fact that these polarons are derived from a narrower Hubbard band. Qualitatively, this fact can be understood in terms of the asymmetric tendency of the system towards phase separation when  $t' \neq 0$  [23]. The polarons also can be understood as an incipient form of phase separation, as the core shows strong ferromagnetic correlations.

Polarons converge in a wide region of the phase diagram, coexisting with AF and dcDW as shown in fig. 2. They have lowest energy in the doping range  $0.007 \leq x \leq 0.035$  ( $1 \leq h \leq 5$ ). They do not converge in the range  $0.076 \leq x \leq 0.097$  ( $11 \leq h \leq 13$ ) where the noncollinear solution has lower energy. This is also different from the situation with  $t' = 0$  where polarons converge and have lower energy in the full range of dopings  $2 \leq h \leq 30$  [8]. The DOS of polarons is shown in fig. 5b for five holes. Fig. 5a shows the reference AF state at half filling. In the DOS for polarons the localized states appear in the antiferromagnetic gap. As doping increases, they form a mid gap subband but the shape of antiferromagnetic spectrum is still clearly seen (see fig. 5c).

### Diagonal commensurate domain-walls

The dcDW configuration is formed by polarons arranged in the diagonal direction creating an almost one dimensional charged wall that forms a ferromagnetic domain (see fig. 4b). We stress “commensurate ” because they do not separate different AF domains as stripes do. The density of states of these solutions differ from that of usual domain walls in that the one dimensional band where the holes are located is wider, and the Fermi level lies inside it. We do not find a size independent one particle gap in these solutions, unlike for conventional domain walls. Within the numerical precision of our calculations, these structures are metallic, while antiphase domain walls are insulating.

The dcDW are the predominant configuration in the AF region. They converge in the range of dopings  $0.014 \leq x \leq 0.118$  ( $2 \leq h \leq 17$ ) and are the minimal energy configuration in most of the doping range as can be seen in fig. 2. These configurations resemble an array of the polarons discussed earlier, along the (1,1) direction. Thus, we can say that individual polarons have a tendency towards aligning themselves along the diagonals. This may be due to the fact that  $t'$  favors the hopping along these directions. This tendency can be also seen in the density of states. We have also checked that a lower value of  $t'$  ( also for  $U = 8$ ) these configurations are less favored. In particular for  $U = 8$ , dcDW are not formed at low  $t'$  while they do form at  $t' = 0.3$ . Moreover we have tried vertical domain walls and they are not formed for  $U = 8$  and  $t' = 0.3$  but they do with  $t'$  lower ( $t' = 0.1$ ). Summarizing, we have checked that  $t'$  favours dcDW against POL and disfavours vertical DW. This behaviour is also found with the striped configurations (see below).

### Non collinear solution $S_x$

The structure denoted by  $S_x$  in the phase diagram consists of a special configuration with noncollinear spin  $S_z$ . It appears in the range of dopings  $0.076 \leq x \leq 0.097$ , ( $11 \leq h \leq 13$ ), in competition with dcDW and has lower energy. We have checked that this structure is never seen in the absence of  $t'$  and is also found at  $U = 4$  and  $t' = 0.3$ .

The configuration is shown in fig. 4c. We see that there are polarons but there is a contribution of the spin  $x$  at some random sites. The convergence in this configuration is very slow. It is interesting to point out that we obtain this configuration when using

conventional polarons as the initial condition.

We do not have a complete understanding of why this configuration is preferred in this region although, it is interesting to note that it happens for the commensurate value of twelve holes (in our  $12 \times 12$  lattice) and the two neighboring values  $h = 11$  and  $h = 13$ .

Its density of states shown in fig. 5d is very similar to the polaronic DOS.

## Stripes

The striped configurations are similar to the domain-walls but the one dimensional arrange of charge separates antiferromagnetic domains with a phase shift of  $\pi$ . Two typical striped configurations are shown in fig. 6a and fig. 6b. Recently the stripes have attracted a lot of interest as the half filled vertical stripes (one hole every second site) are found in cuprates while diagonal stripes are found in nickelates [24].

We have obtained stripes as higher energy configurations and we have not found half filled vertical stripes in agreement with other works using mean field approximations for  $U = 8$  [5, 6, 7, 8, 17]. It is known that the addition of a long range Coulomb interaction could stabilize the vertical stripes as ground states for large  $U$  [25] and applying a slave-boson version of the Gutzwiller approach the half filled vertical stripes can be ground states depending on parameters [26].

We have studied the filled vertical stripe and the diagonal stripe obtained at values of the doping commensurate with the lattice. Our main interest is the role played by  $t'$  in these configurations. We have seen that  $t'$  has a strong influence on them:  $t'$  reduces significantly the basin of attraction of the vertical stripes, what agrees with recent calculations in the  $tt' - J$  model [27], while it favors diagonal stripes. The evolution of the vertical stripe with  $t'$  can be seen in fig. 6b and fig. 6c for the values  $U = 4$ ,  $t' = 0$  and  $t' = 0.2$ . These stripes do not converge for higher values of  $t'$ . We have instead found that diagonal stripes are favored by  $t'$  much as the dcDW were.

The density of states of the stripes is very similar to that of polarons. We can conclude that they are insulating states (see fig. 7) unlike the similar commensurate domain walls where a more metallic character can be appreciated.

## 3.2 The ferromagnetic region

The existence of metallic ferromagnetism in the Hubbard model remains one of the most controversial issues in the subject [28]. Large areas of ferromagnetism in the doping parameter were found in the earliest works on the  $t - t'$  Hubbard model within mean field approximation [14] and were often assumed to be an artifact of the approximation which would be destroyed by quantum corrections. There are two main regions where ferromagnetism is likely to be the dominant configuration. One is the region close to half filling, in particular at one hole doping where the Nagaoka theorem ensures a fully polarized ferromagnetic state in a bipartite lattice at  $U = \infty$ . The other is the region around the Van Hove fillings where there is a very flat lower band and where ferromagnetism was found for large

values of  $t'$  close to  $t' = 0.5$  with quantum Monte Carlo techniques [9] and in the T-matrix approximation [10]. FM is also found to be the dominant instability for small  $U$  and large  $t'$  in analytical calculations based on the renormalization group [11], and at intermediate values of  $U$  with a mixture of analytical and mean field calculations [29]. Finally, there is a controversy on whether Nagaoka ferromagnetism is stabilized at the bottom of the band  $\rho \rightarrow 0$  [30].

Most of the previous calculations relay on the study of the divergences of the magnetic susceptibility pointing to either a symmetry breaking ground state or to the formation of spin density waves as low energy excitations of the system. In many cases it is not possible in this type of analyses to discern on the precise nature of the magnetic phases, and, in particular, whether they correspond to fully polarized states (long range order) or to inhomogeneous configurations with an average magnetization. A complete study of the magnetic transitions as a function of the electronic density is also a difficult issue.

We have studied the stability of ferromagnetic configurations in the full range of dopings discussed previously. Two main issues can be addressed within the method of the present paper. One is the existence of the fully polarized ferromagnetic state (Nagaoka state), and its stability not only towards the state with one spin flip, but against any weakly polarized or paramagnetic configuration. The other is the specific symmetry of the partially polarized ferromagnetic configurations.

In the region close to half filling, our results indicate that the Nagaoka theorem does probably hold in the presence of  $t'$  (which spoils the bipartite character of the lattice) since the Nagaoka state appears when doping with one hole at such large values of  $U$  as to make the kinetic term quite irrelevant. We found Nagaoka FM at values of  $U$  such as  $U = 128$ . No FM configurations are found doping with two holes even at  $U = 128$ .

The region of low to intermediate electron density has been analyzed for various values of  $U$  and  $t'$ . This region includes dopings close to the Van Hove singularity where FM should be enhanced due to the large degeneracy of states in the lower band. The position of the Van Hove singularity for a given value of  $U$  and  $t'$  can be read off from the undoped DOS; it has been determined in [31]. Our results are the following:

Nagaoka FM is not found for  $t' = 0.1$  at any filling for  $U \leq 8$ . For  $t' = 0.3$ , two types of FM configurations are the most stable in the range of dopings shown in fig. 1. Ferromagnetic spin density waves (fm SDW) depicted in fig. 8b dominate the phase diagram at densities close to the AFM transition  $0.146 \leq x \leq 0.194$  ( $21 \leq h \leq 28$ ), and in  $x \geq 0.264$  ( $h \geq 37$ ). In the region in between, ferromagnetic domains (fm DOM) as the one shown in fig. 8c are the most stable. Both types of configurations show a strong charge segregation and are clearly metallic. The excitation spectrum of these configurations can be seen in fig. 9.

Fully polarized FM metallic states (Nagaoka) shown in fig. 8a, are found at all values of  $h$  corresponding to closed shell configurations from a critical value  $h_c(U)$  depending on  $t'$  till the bottom of the band. They are shown as vertical solid lines in fig. 1. They are



also metallic with a higher DOS at the Fermi level than the partially polarized configurations. Larger values of  $t'$  or  $U$  push down the critical  $h$  in agreement with previous works [14, 10]. Some values of  $h_c(U)$  are, for  $t' = 0.3$ ,  $h_c(6) = 37$ ,  $h_c(8) = 29$ ,  $h_c(10) = 21$ . For  $t' = 0.4$ ,  $h_c(8) = 25$ . As mentioned before, no FM is found for  $t' = 0.1$ .

The former results show a large region of ferromagnetic configurations whose upper boundary coincides with previous estimations [10] but which extends to the bottom of the band. We have found paramagnetic configurations to converge in the bottom of the band but their energies are higher than the ferromagnetic ones. Comparing our solutions with the corresponding results obtained with the same method in the case  $t' = 0$  [8], we find that the inclusion of  $t'$  favors ferromagnetism for intermediate to large dopings.

### 3.3 Phase separation

Although the issue of phase separation (PS) in the Hubbard model is quite old [32], it has become the object of very active research work [33] following the experimental observation of charge segregation in some cuprates [34]. Despite the effort, the theoretical situation is quite controversial, although recent calculations rule out PS in the 2D Hubbard model [35, 16]. It seems to occur above some values of  $J$  [36, 37, 38], although other work suggests that it is likely for all values of  $J$  in the  $t - J$  model [39]. PS has also been invoked in connection with the striped phase of the cuprates [40].

The theoretical study of PS is a difficult subject. While it is a clear concept in statistical mechanics dealing with homogeneous systems in thermodynamical equilibrium, the characterization of PS in discrete systems is much more involved. It is assumed to occur in those density regions where the energy as a function of density is not a convex function. This behavior is difficult to achieve in finite systems where the indication of PS is a line,  $E(x)$ , of zero curvature, i.e. of infinite compressibility. Even this characterization, which should be correct if it refers to uniform phases of the system, is problematic when many inhomogeneous phases compete in the same region of parameter space. On the other hand, simple thermodynamic arguments suggest that it should be a general phenomenon near magnetic phase transitions [41].

PS is also very hard to observe numerically as demonstrated by the results cited previously. Exact results as the one obtained in [35] are very restrictive and hence of relative utility.

Our work supports the evidence for phase separation of the model in several ways. The first is through the plot of the total energy of the minimal energy configuration as a function of the doping  $x$  shown in fig. 1. There we can see that the dominant feature follows a straight line. As mentioned before, this characterization has the problem of comparing the energies of different type of configurations.

The evidence is more clear if we observe the same plot for a given fixed configuration in the AF region where phase separation occurs (fig. 2). The polaronic configurations in fig. 2 follow a straight line while negative curvature is clearly seen in the plot of the commen-

surate domain walls, the more abundant solution in this region. A Maxwell construction done to this region of curve interpolates rather well to half filling.

The best evidence is provided by the comparison between the plots corresponding to the two uniform configurations existing in the system. In the case of the Nèel state (AF of fig. 2) we can see a straight line in the region of densities where it is a self-consistent solution. This plot should be compared with the one in fig. 10 corresponding to the uniform Nagaoka states. In the large region where this homogeneous state is found, the plot follows very closely a standard quadratic curve.

Finally we have looked at the charge and spin configurations of minimal energy. Apart from the AFM configuration at half filling and the Nagaoka FM, all inhomogeneous configurations show the same path: coexisting regions of an accumulation of holes accompanied by a ferromagnetic order with regions of lower density with an AFM order. The charge segregation is obvious in configurations like the ones shown in fig. 4 and in fig. 8c.

We have found fully polarized solutions in closed shell configurations down to the lowest electron occupancies allowed in our  $12 \times 12$  cluster (5 electrons). However, we cannot rule out the existence of paramagnetic solutions at even lower fillings.

With all the previous hints we reach the conclusion that the  $t - t'$  Hubbard model tends to phase separate into an antiferromagnetic and a ferromagnetic fully polarized state with different densities for any doping away to half filling up to the Van Hove filling where FM sets in. It is interesting to note that this result was predicted in a totally different context by Markiewicz in ref. [42]. Phase separation has also been predicted in the same range of dopings in ref. [10] but between a paramagnetic and a ferromagnetic state.

## 4 Conclusions

In this paper we have analyzed the charge and spin textures of the ground state of the  $t - t'$  Hubbard model in two dimensions as a function of the parameters  $U$ ,  $t'$  and the electron density  $x$  in a range from half filling to intermediate hole doping with the aim of elucidating the role of  $t'$  on some controversial issues. These include the existence and stability of ordered configurations such as domain walls or stripes, and the magnetic behavior in the region of intermediate to large doping where the lower band becomes very flat.

We have used an unrestricted Hartree Fock approximation in real space as the best suited method to study the inhomogeneous configurations of the system.

Our results are summarized in the representative phase diagram of fig. 1 obtained for the standard values of the parameters  $U = 8$ ,  $t' = 0.3$ . There we can see that the system undergoes a transition from generalized antiferromagnetic insulating configurations including spin polarons and domain walls, to metallic ferromagnetic configurations. For the values of the parameters cited, the transition occurs at an electron density  $x = 0.125$  ( $h = 18$ ). Both types of magnetic configurations converge in the intermediate region indicating that

the transition is smooth more like a crossover.

The generalized antiferromagnetic configurations are characterized by a large peak in the density of states of the lower band and by the presence of an antiferromagnetic gap with isolated polarons for very small doping that evolves to a mid gap subband for larger dopings. ferromagnetic configurations have a metallic character with a DOS at the Fermi level that increases for configurations with increasing total magnetization. Fully polarized Nagaoka states are found at all closed shell configurations in the ferromagnetic zone of the phase diagram. They have the highest DOS at the Fermi level.

Apart from the homogeneous Néel and Nagaoka states, all inhomogeneous configurations show the existence of the two magnetic orders associated to charge segregation. AF is found in the regions of low charge density and FM clusters are formed in the localized regions where the extra charge tends to accumulate.

Our main conclusion is that the only stable homogeneous phases of the system consists of the purely antiferromagnetic Néel configuration at half filling, and Nagaoka ferromagnetism, which appears around the Van Hove filling. We find the system is unstable towards phase separation for all intermediate densities.

We have reached this conclusion through a careful study of the curves representing the total energy versus doping of the various configurations. Besides, the approach used allows us to visualize the inhomogeneous configurations. In all of them we find coexisting regions of an accumulation of holes accompanied by a ferromagnetic order with regions of lower density with an antiferromagnetic order.

As the ferromagnetic phase is metallic while the Néel state is insulating, we expect the transport properties of the model in the intermediate region to resemble that of a percolating network, a system which has attracted much attention lately [43, 44].

Finally, our study does not exclude the existence of other non magnetic instabilities, most notably d-wave superconductivity. This can be, however, a low energy phenomenon, so that the main magnetic properties at intermediate energies or temperatures are well described by the study presented here.

We thank R. Markiewicz for a critical reading of the manuscript with very useful comments. Conversations held with R. Hlubina, E. Louis, and M. P. López Sancho are also gratefully acknowledged. This work has been supported by the CICYT, Spain, through grant PB96-0875 and by CAM, Madrid, Spain.

## References

- [1] P.W. Anderson, Science **235**, 1196 (1987).
- [2] P. Bénard, L. Chen and A. M. Tremblay, Phys. Rev. B. **47**, 15 217 (1993); Q. Si, T. Zha, K. Levin and J. P. Lu, *ibid.* **47**, 9055 (1993).
- [3] A. Nazarenko et al., Phys. Rev. **B 51**, 8676 (1995).
- [4] Y. Maeno et al., Nature **372**, 532 (1994).
- [5] W. P. Su, Phys. Rev. **B 37**, 9904 (1988).
- [6] D. Poilblanc and T.M. Rice, Phys. Rev. **B 39**, 9749 (1989).
- [7] M. Inui and P.B. Littlewood, Phys. Rev. **B 44**, 4415 (1991).
- [8] J. A. Vergés, E. Louis, P. S. Lombdahl. F. Guinea, and A. R. Bishop, Phys. Rev. **B 43**, 6099 (1991).
- [9] R. Hlubina, S. Sorella, and F. Guinea, *Phys. Rev. Lett.* **78**, 1343 (1997).
- [10] R. Hlubina, Phys. Rev. **B 59**, 9600 (1999).
- [11] J. V. Alvarez, J. González, F. Guinea, and M. A. H. Vozmediano, J. Phys. Soc. Japn. **67**, 1868 (1998).
- [12] E. Louis, F. Guinea, M. P. López-Sancho and J. A. Vergés, Europhys. Lett. **44**, 229 (1998).
- [13] E. Louis, F. Guinea, M. P. López-Sancho and J. A. Vergés, Phys. Rev. B, **59**, 14005 (1999).
- [14] H. Q. Lin and J. E. Hirsch, Phys. Rev. **B 35**, 3359 (1987).
- [15] M. P. López Sancho, J. Rubio, M. C. Refolio, and J. M. López Sancho, Phys. Rev. **B 46**, 11110 (1992).
- [16] A. C. Cosentini, M. Capone, L. Guidoni, and G. B. Bachelet, Phys. Rev. B **58**, R14685 (1998).
- [17] J. Zaanen and O. Gunnarson, Phys. Rev. B **40**, 7391 (1989).
- [18] H. J. Schulz, Phys. Rev. Lett. **64**, 1445 (1990).
- [19] M. Imada, A. Fujimori and Y. Tokura, Rev. Mod. Phys. **70**, 1039 (1998).
- [20] J. R. Schrieffer, X. -G. Wen, and S. -C. Zhang, Phys. Rev. Lett. **60**, 943 (1988).
- [21] W. Hofstetter and D. Vollhardt, Ann. Physik **7**, 48 (1998).
- [22] G. Seibold, E. Sigmund, and V. Hizhnyakov, Phys. Rev. B **57**, 6937 (1998).

- [23] F. Guinea, E. Louis, M. P. López-Sancho and J. A. Vergés, *Universality Class of the Antiferromagnetic Transition in the Two Dimensional Hubbard Model*, preprint (cond-mat/9901164).
- [24] J. M. Tranquada, B. J. Sternlieb, J. D. Axe, Y. Nakamura and S. Uchida, *Nature* **375**, 561 (1995); J. M. Tranquada, J. D. Axe, N. Ichikawa, A. R. Moodenbaugh, Y. Nakamura and S. Uchida, *Phys. Rev. Lett.* **78**, 338 (1997).
- [25] J. Zaanen and M. Oleś, *Ann. Physik* **5**, 224 (1996).
- [26] G. Seibold, C. Castellani, C. Di Castro and M. Grilli, *Phys. Rev. B* **58**, 13506 (1998).
- [27] S. R. White, and D. J. Scalapino cond-mat/9812187.
- [28] For a recent review with a complete list of references see: D. Volhardt, N. Blümer, K. Held, M. Kollar, J. Schlipf, M. Ulmke, and J. Wahle, *Z. Phys. B* **103**, 283 (1997).
- [29] M. Murakami and H. Fukuyama, *J. Phys. Soc. Japn.* **67**, 2784 (1998); M. Murakami, *Possible ordered states in the 2D Hubbard model*, cond-mat/9904213.
- [30] T. Hanish, G. S. Uhrig, and E. Müller-Hartmann, *Phys. Rev. B* **56**, 13 960 (1997). See also T. Hanish, G. S. Uhrig, and E. Müller-Hartmann, *Lattice dependence of ferromagnetism in the Hubbard model*, cond-mat/9707286.
- [31] A. Avella, F. Mancini, D. Villani, and H. Matsumoto, *Physika C* **282-287**, 1759 (1997).
- [32] P. B. Visscher, *Phys. Rev. B* **10**, 943 (1974).
- [33] For an overview of the subject, see K. A. Müller, and G. Benedek, eds., *Proceed. of the conf. Phase separation in cuprate superconductors*, World Scientific (1993).
- [34] J. D. Jorgensen et al., *Phys. Rev. B* **38**, 11 337 (1988); D. R. Harshman et al., *Phys. Rev. Lett.* **63**, 1187 (1989).
- [35] G. Su, *Phys. Rev. B* **54**, R8281 (1996).
- [36] V. J. Emery, S. A. Kivelson, and H. Q. Lin, *Phys. Rev. Lett.* **64**, 475 (1990).
- [37] E. W. Carlson, S. A. Kivelson, Z. Nussinov and V. J. Emery, *Phys. Rev. B* **57**, 14704 (1998).
- [38] M. Calandra, F. Becca and S. Sorella, *Phys. Rev. Lett.* **81**, 5185 (1998).
- [39] C. S. Hellberg, and E. Manousakis, *Phys. Rev. Lett.* **78**, 4609 (1997).
- [40] J. M. Tranquada et al., *Phys. Rev. Lett.* **78**, 338 (1997).
- [41] F. Guinea, G. Gómez-Santos and D. Arovas, cond-mat/9907184 (preprint).
- [42] R. S. Markiewicz, *J. Phys. Cond. Matt.* **2**, 665 (1990).
- [43] E. Shimshoni and A. Auerbach, *Phys. Rev. B* **55**, 9817 (1997).
- [44] E. Shimshoni, A. Auerbach and A. Kapitulnik, *Phys. Rev. Lett.* **80**, 3352 (1999).

## 5 Figure captions

Fig. 1: Complete phase diagram for  $U = 8$ ,  $t' = 0.3$ . Vertical dashed lines separate the different configurations described in the text. Vertical solid lines correspond to closed shells fillings where Nagaoka ferromagnetism occurs. The curve is a plot of the total energy (in units of  $t$ ) of the lowest energy configuration versus the electron density  $x$ .

Fig. 2: Comparison between the energies of the different configurations converging in the AF region. The configurations are displayed in fig. 4.

Fig. 3: Comparison between the energies of the configurations in the FM region. The configurations are displayed in fig. 8.

Fig. 4: Examples of the minimal energy configurations discussed in the text for the reference values  $U=8$ ,  $t'=0.3$  in the antiferromagnetic region. Fig. 4a shows the polaronic (POL) configuration obtained when doping with five holes. Fig. 4b shows the diagonal commensurate domain wall (dcDW) configuration doping with six holes. Fig. 4c shows non collinear ( $S_x$ ) configuration obtained when doping with twelve holes.

Fig. 5: Density of states of the various configurations discussed in the text in the antiferromagnetic region for the parameter values  $U = 8$ ,  $t' = 0.3$ . The fermi level is indicated as a vertical line. Fig. 5a shows the reference Néel configuration at half filling. The asymmetry of the band due to  $t'$  is noticeable. The rest of figures show POL with 5 holes (5b), POL with 14 holes (5c), dcDW with 6 holes (5d), and the  $S_x$  configuration with 12 holes (5e).

Fig. 6: Striped configurations appearing at values of the doping commensurate with the lattice. Fig. 6a. shows the diagonal stripe obtained for the parameter values  $U = 8$  and  $t' = 0.3$ . Figs. 6b and 6c correspond to a vertical stripe obtained for  $U = 4$  for the values of  $t'$   $t' = 0$  (6b), and  $t' = 0.2$  (6c). We can see that for bigger  $t'$  the vertical stripe is spoiled.

Fig. 7: Density of states of the diagonal stripe configurations. The Fermi level is indicated as a vertical line.

Fig. 8: Examples of the minimal energy configurations discussed in the text for the reference values  $U=8$ ,  $t'=0.3$  in the ferromagnetic region. Fig. 8a shows the fully polarized Nagaoka state (Ng) with  $h=49$ , fig. 8b shows fmSDW obtained for  $h=24$ , and fig. 8c corresponds to the fm DOM obtained for  $h=36$ .

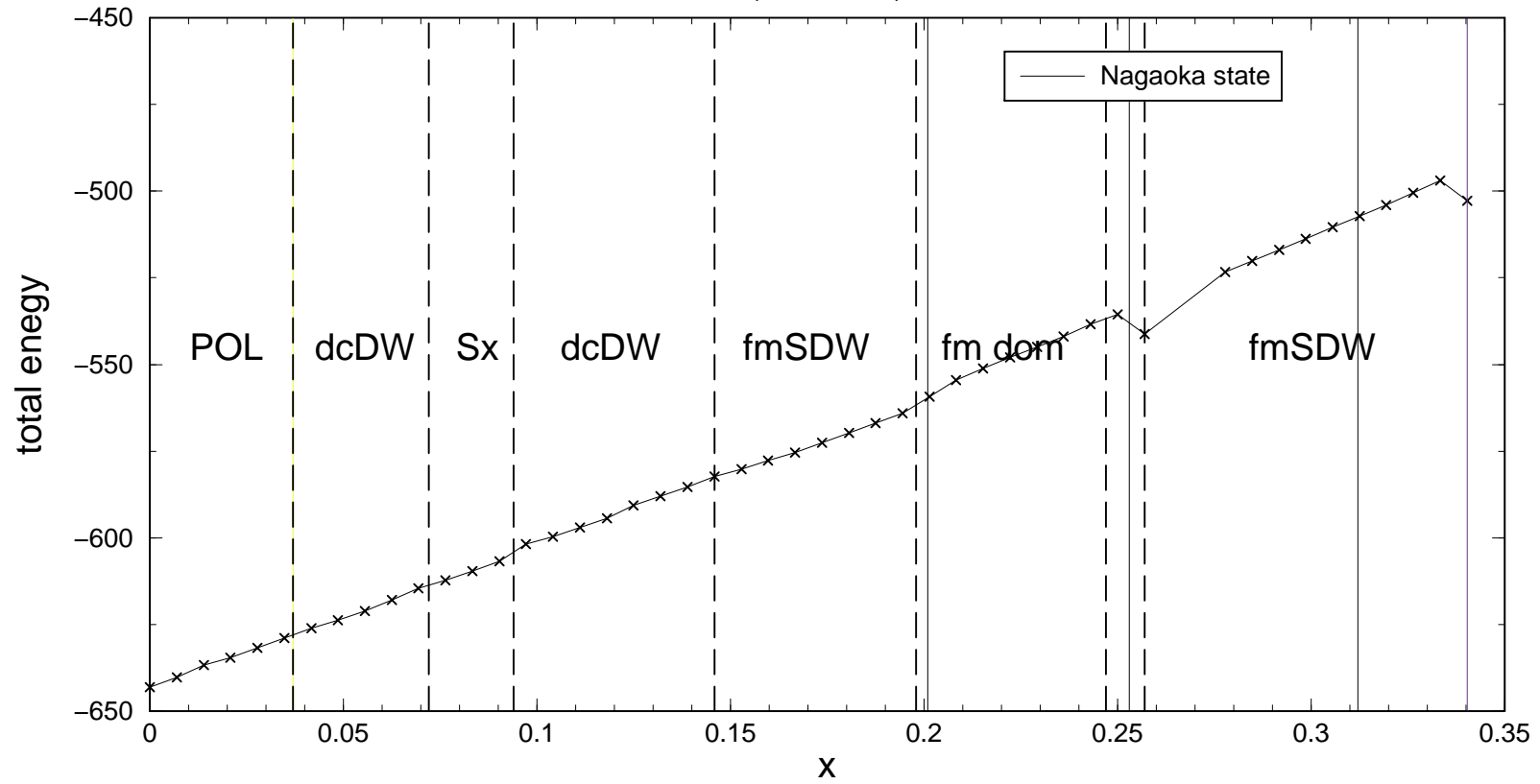
Fig. 9: Density of states of the ferromagnetic configurations in fig. 8. Fig. 9a corresponds to the Nagaoka configuration, fig. 9b to fmSDW, and fig. 9c shows the DOS of FM dom. The Fermi level is indicated as a vertical line.

Fig. 10: Plot of the energy versus doping for the fully polarized Nagaoka configurations in the full range of dopings where they converge. The solid line is a fit to a quadratic curve.

[illegible]

# Total energy versus doping

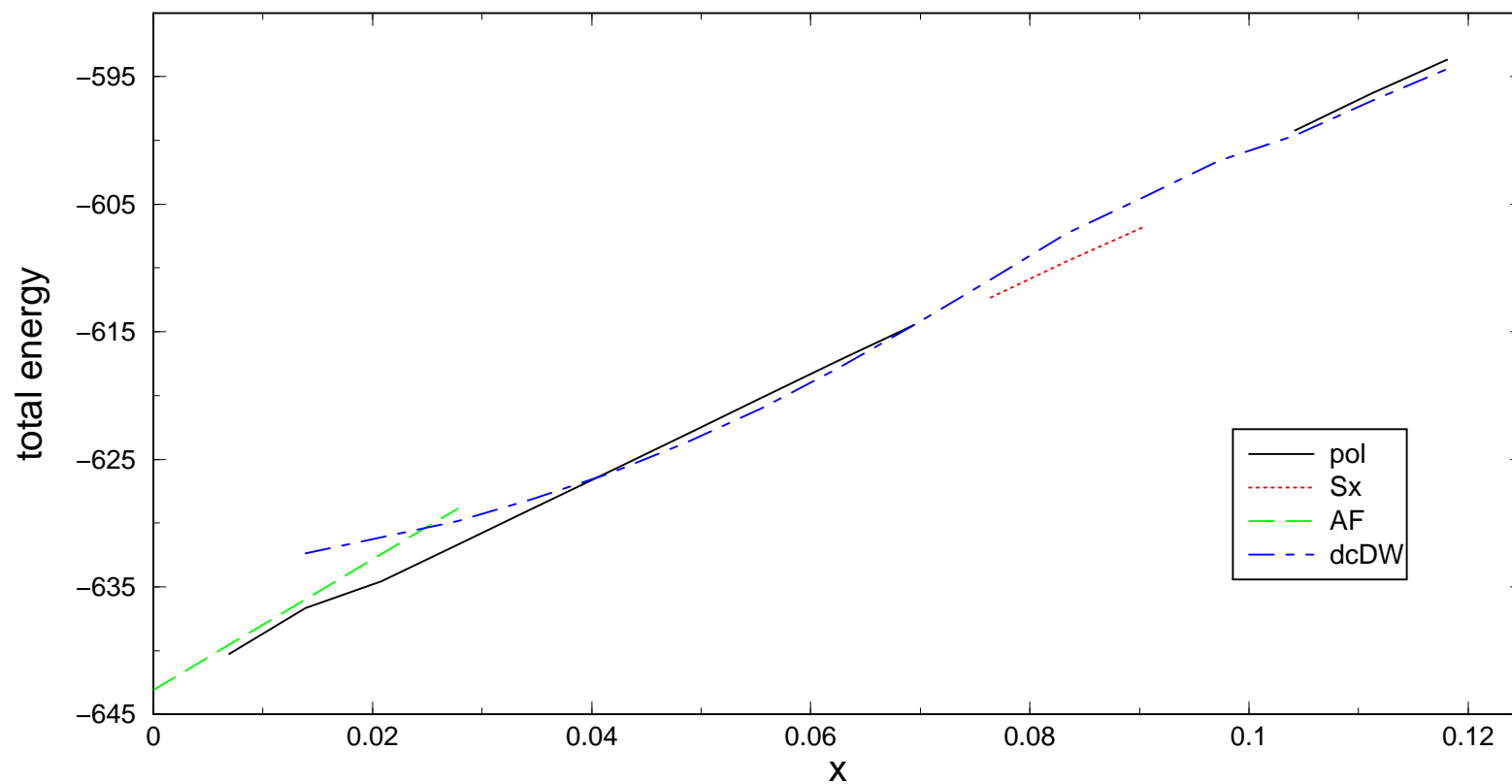
( $U=8, t'=0.3$ )



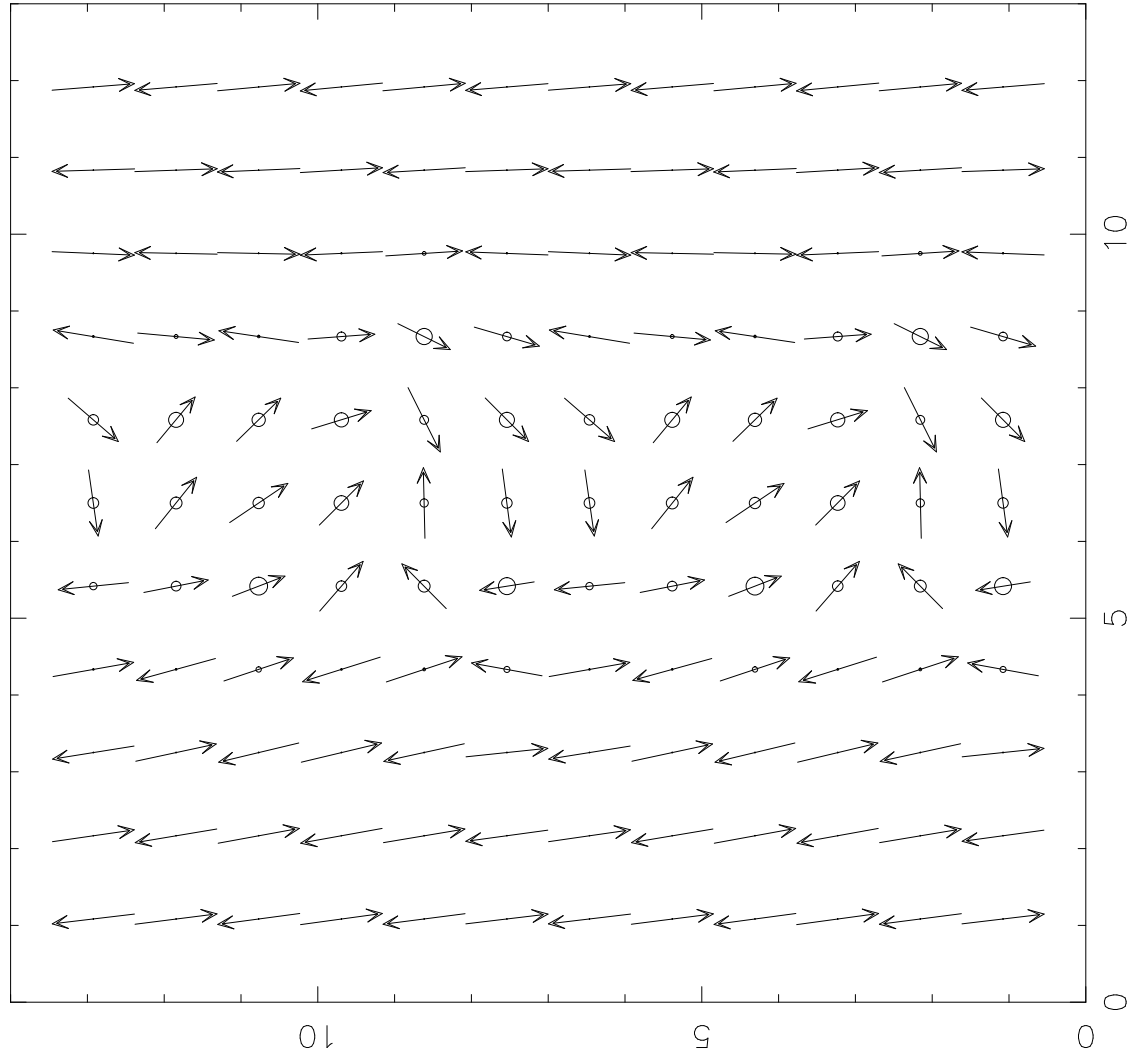


# Energies of different configurations in the AF region

( $U=8, t'=0.3$ )

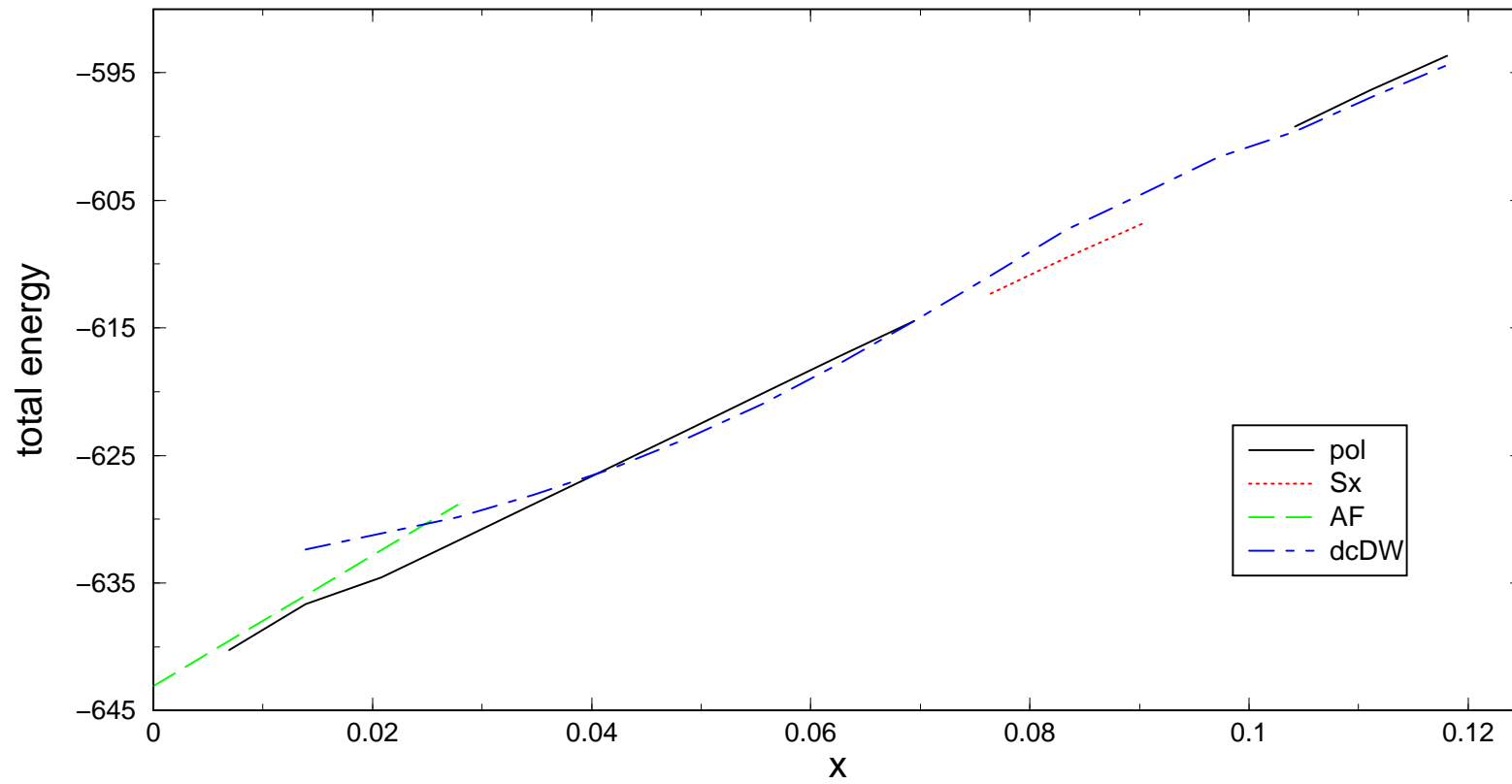


vertical stripe,  $h=12$ ,  $U=4$ ,  $t_2=0.2$

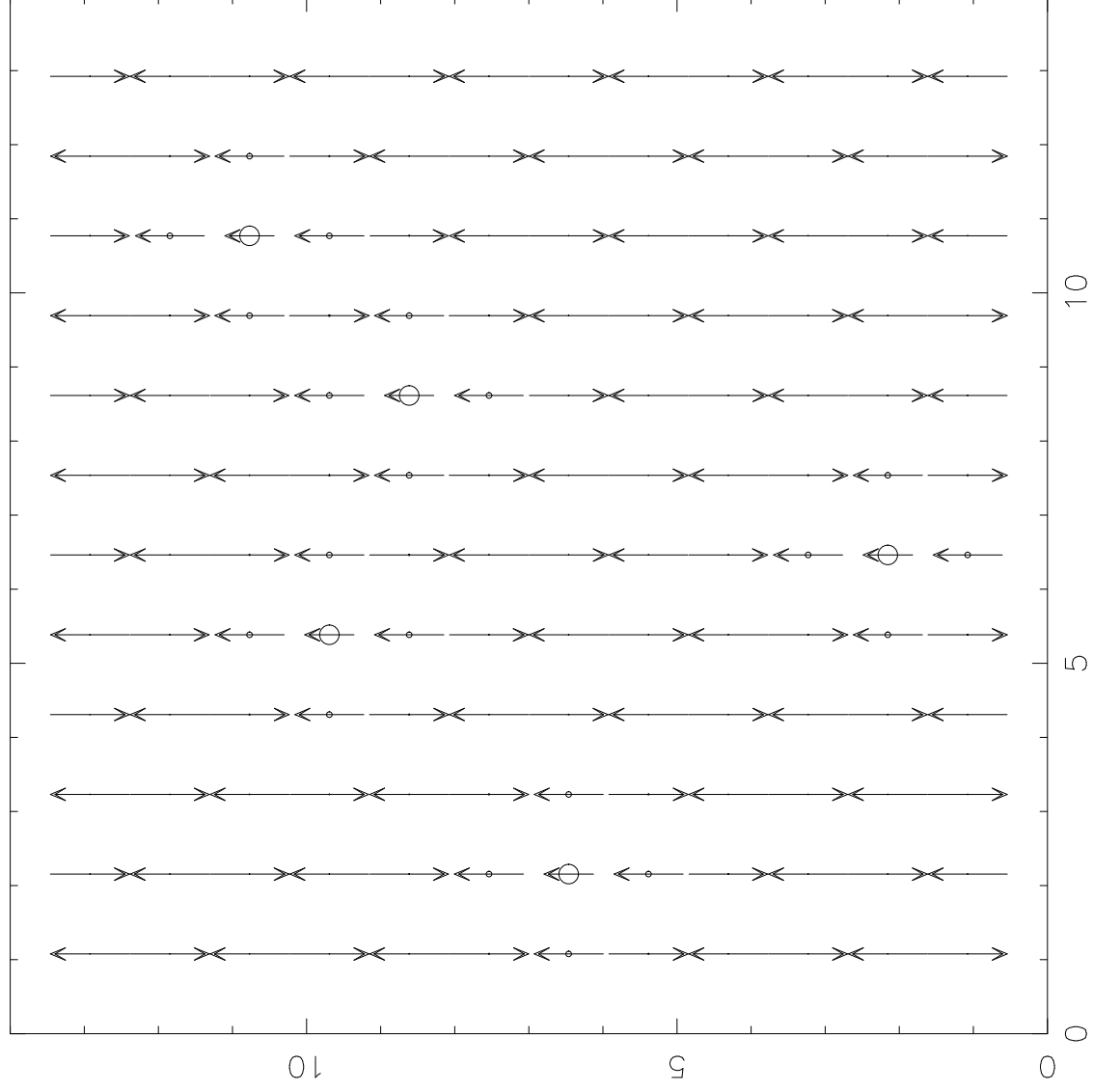


# Energies of different configurations in the AF region

( $U=8, t'=0.3$ )

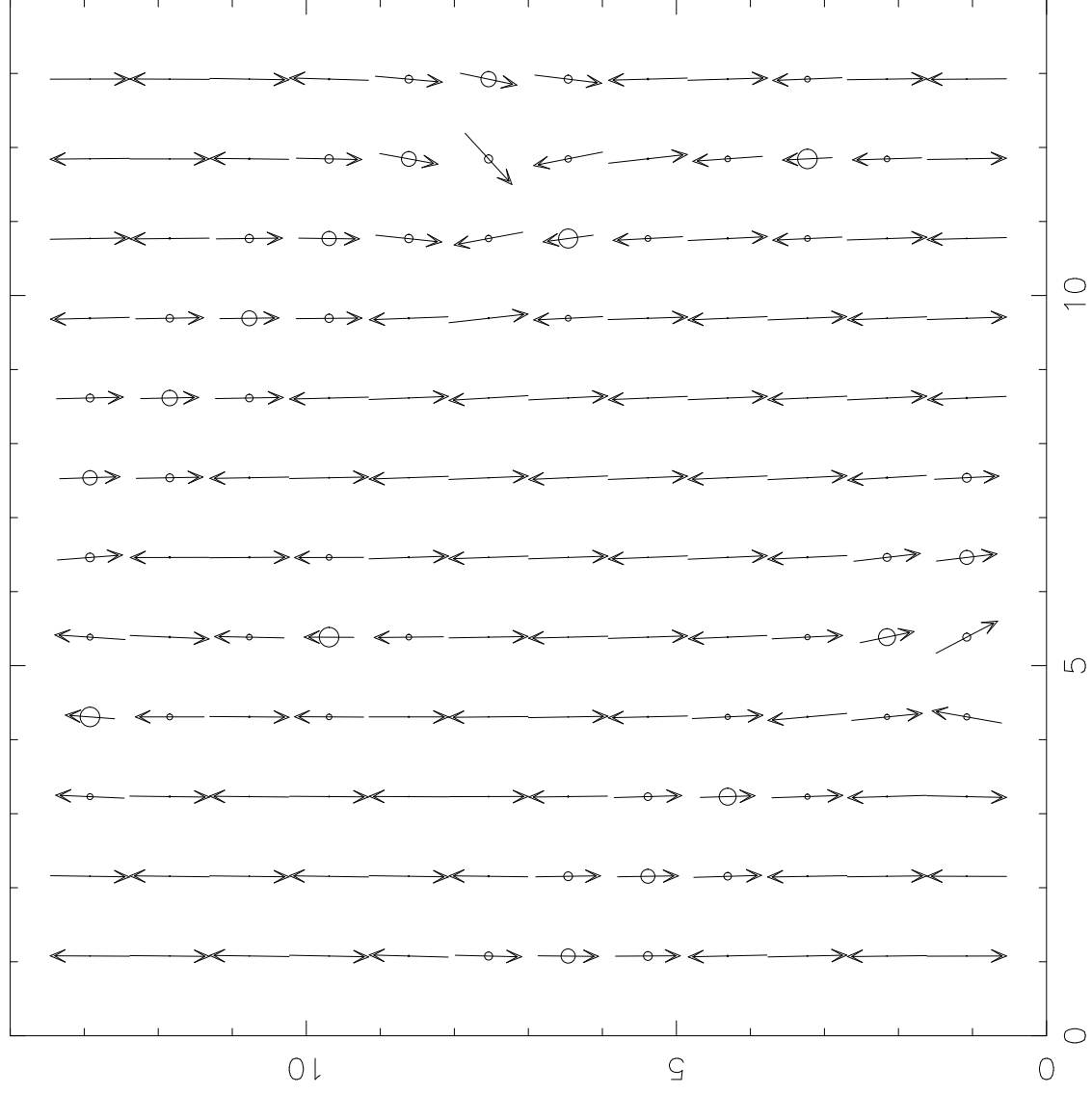


polarons ,  $h=5$ ,  $U=8$ ,  $t_2=0.3$



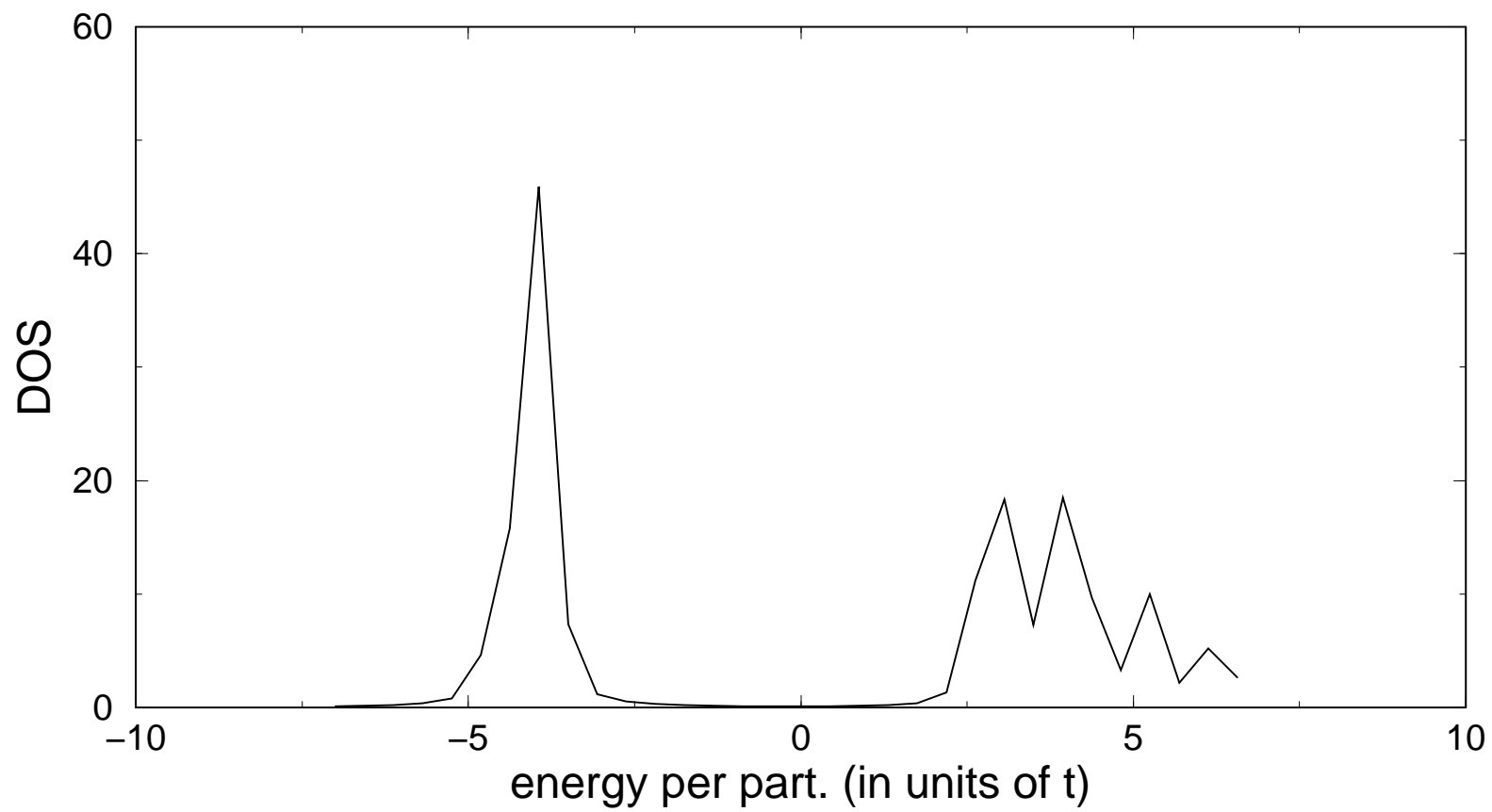


non-collinear  $S_x$ ,  $h=12$ ,  $U=8$ ,  $t_2=0.3$



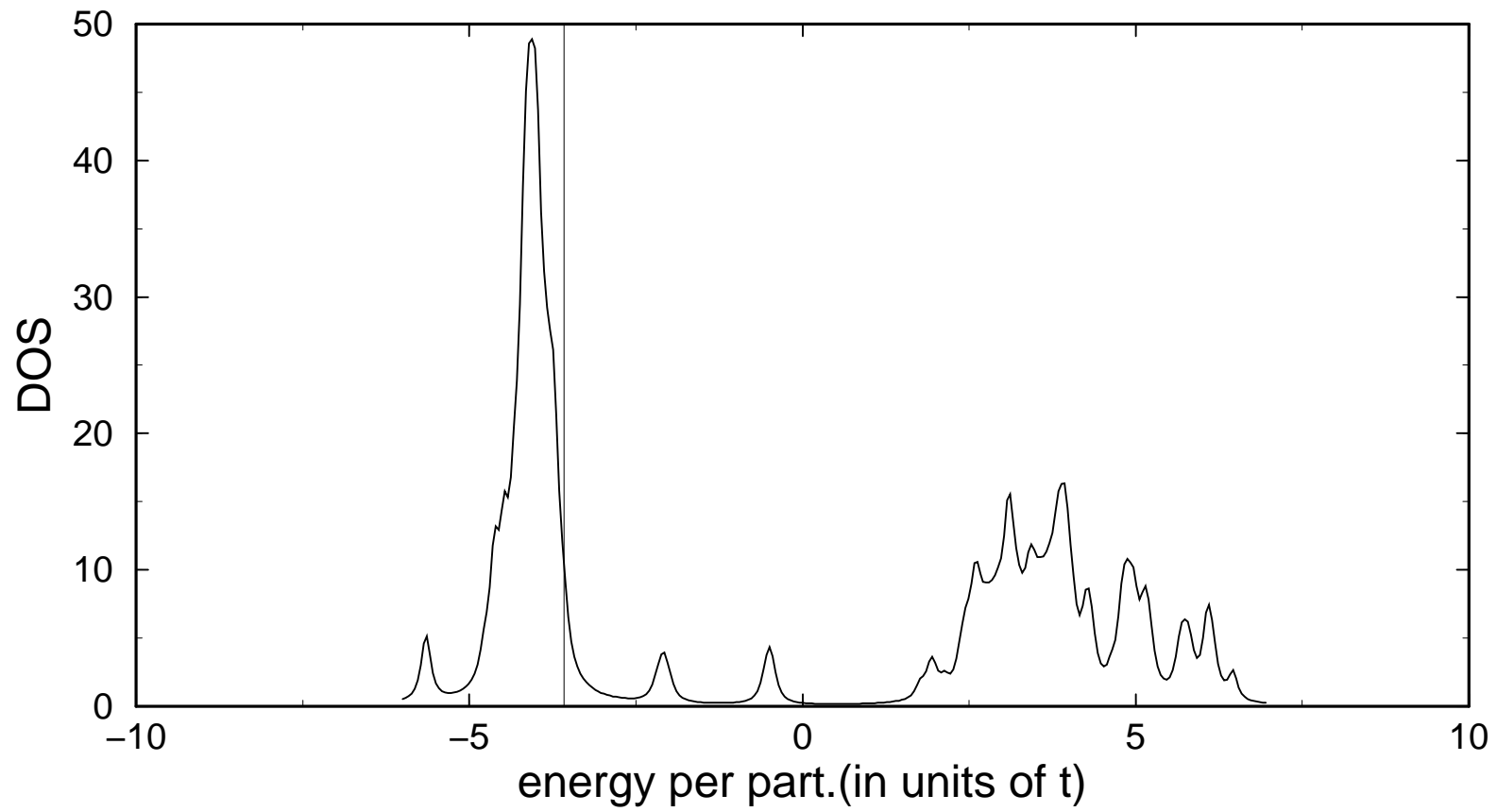
# DOS of AF

( $U=8$ ,  $t'=0.3$ , 0 holes)



# Density of states of polarons

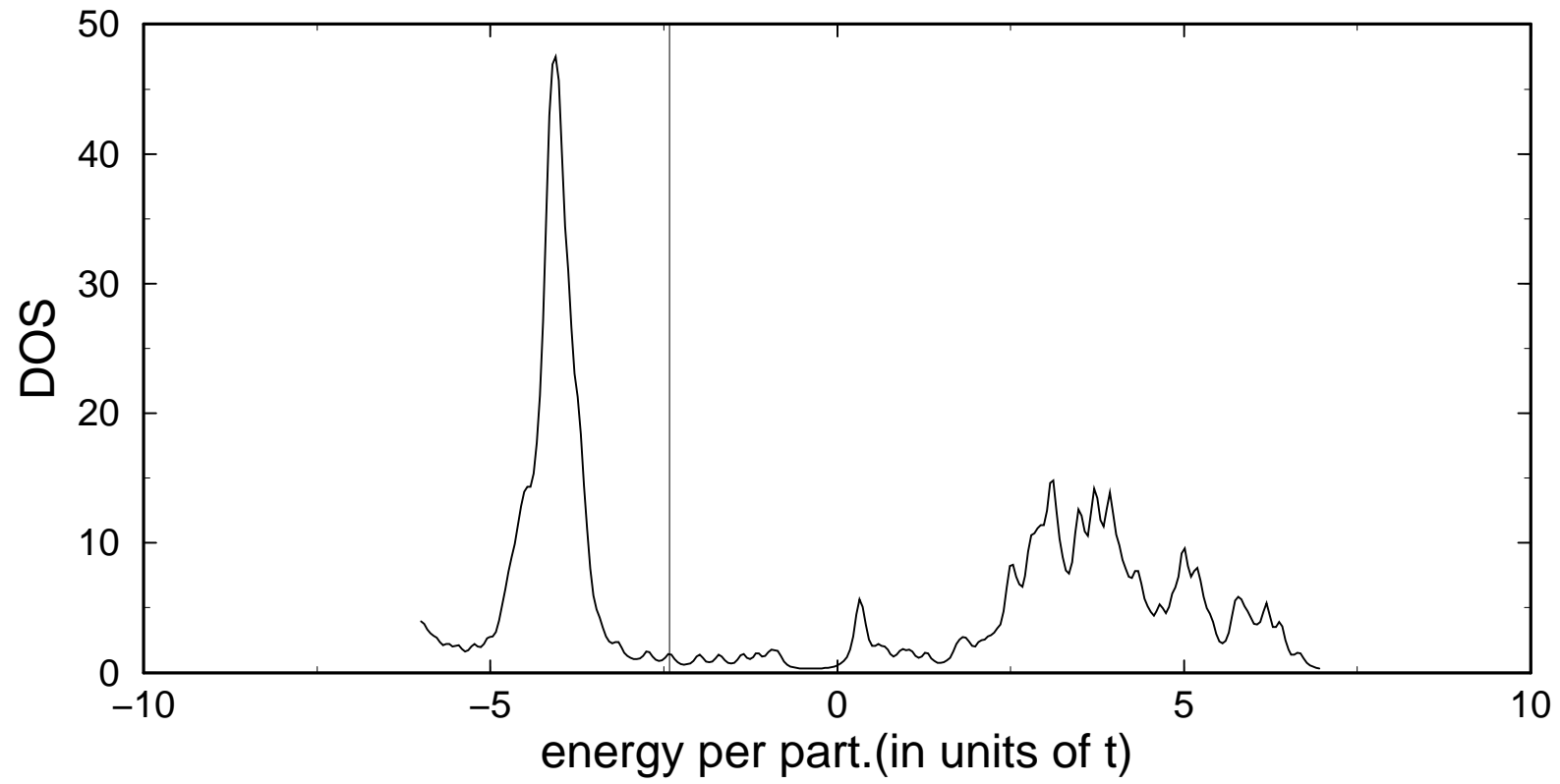
$U=8$ ,  $t'=0.3$ ,  $h=5$





# Density of states of dcDW

$U=8, t'=0.3, h=6$



# Density of states of $S_x$

$U=8, t'=0.3, h=12$

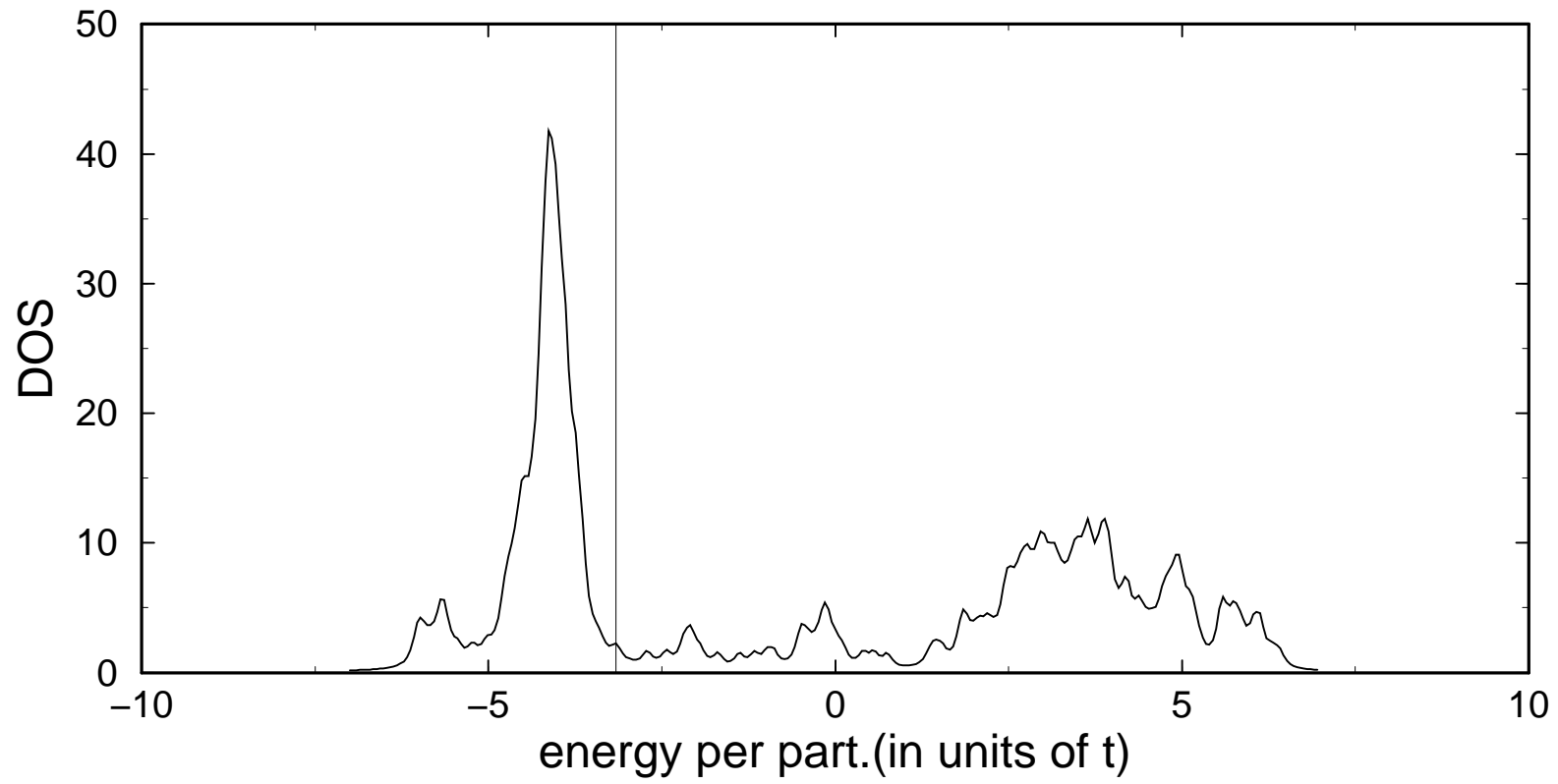
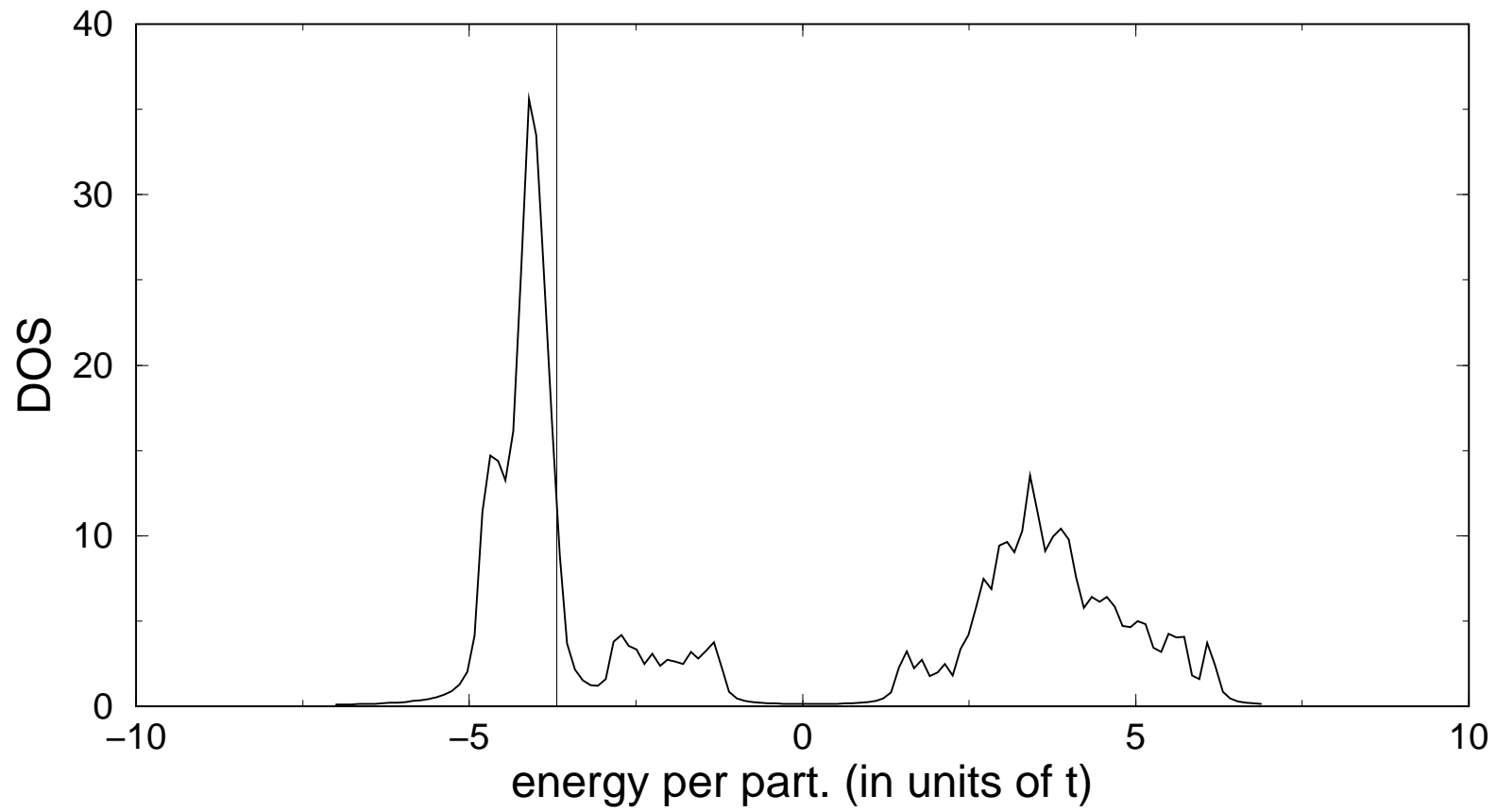
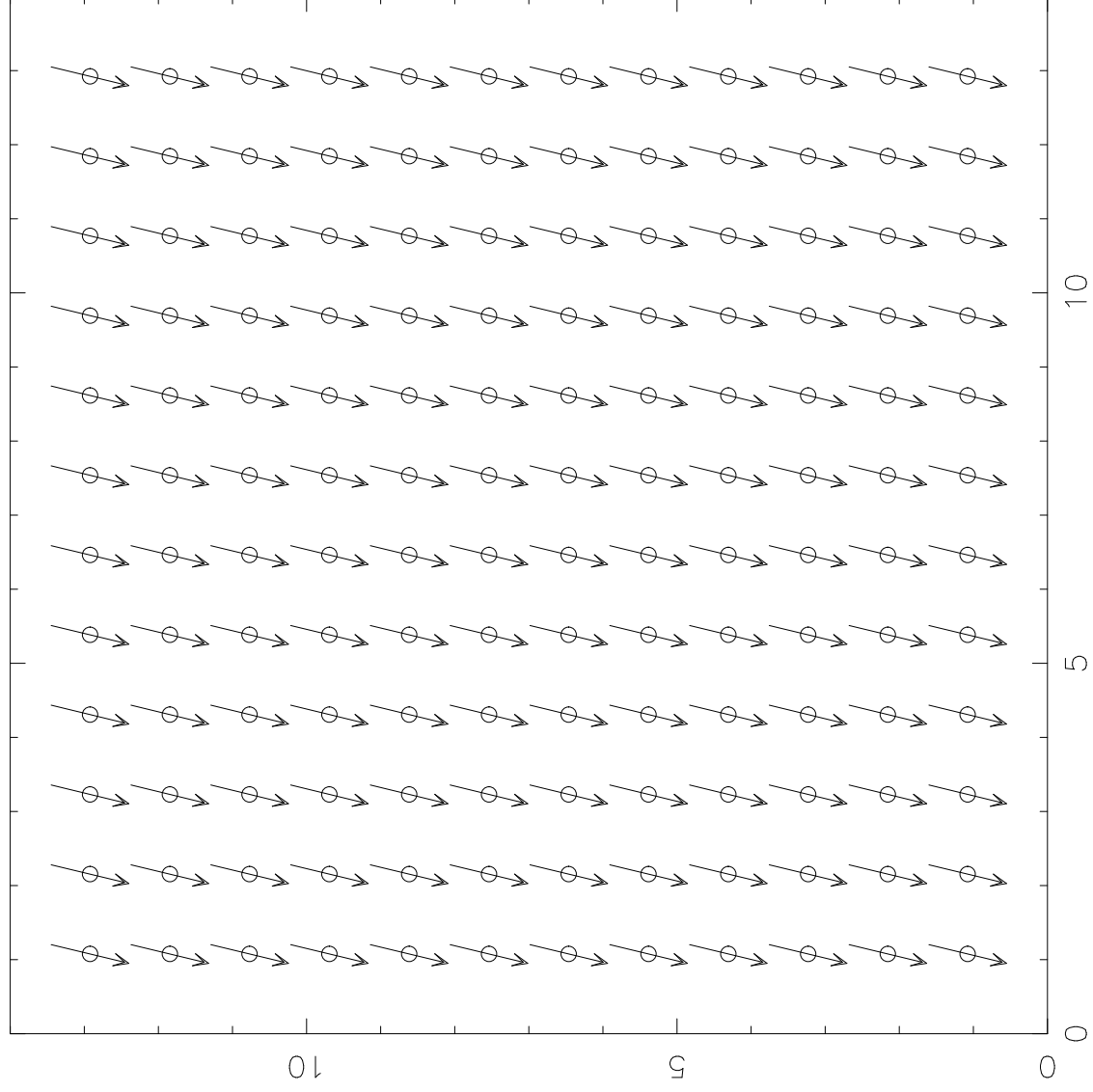


Figure 1 displays a 10x10 grid of diagrams representing the 100 elements of the Coxeter group  $B_{10}$ . The horizontal axis is labeled 0 to 10, and the vertical axis is labeled 0 to 10. Each diagram consists of horizontal lines with arrows and circles, representing different elements of the group. The diagrams are arranged in a grid where each row and column contains 10 distinct elements.

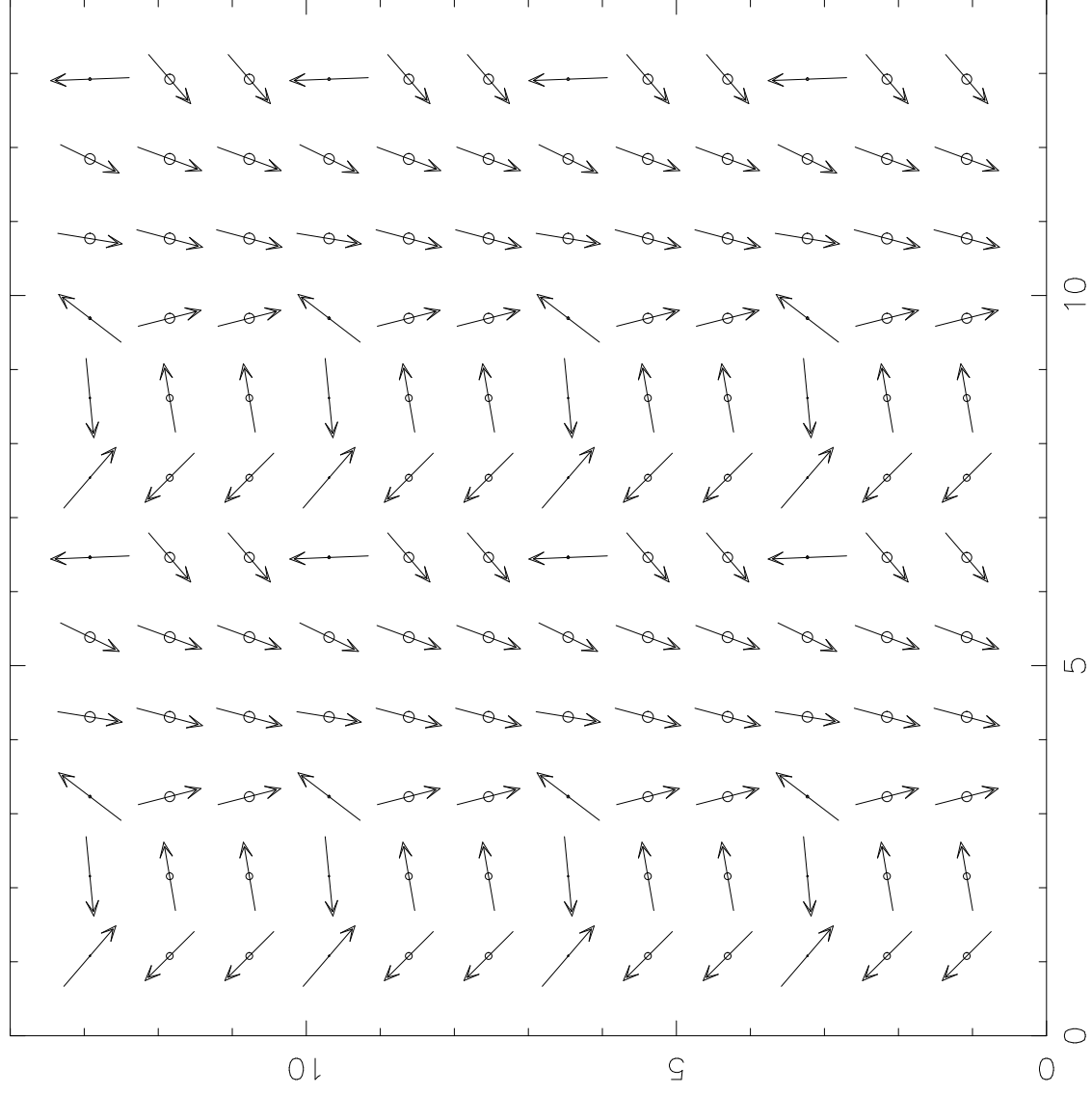
DOS of diagonal stripes  
( $U=8$ ,  $t'=0.3$ , 11 holes, 11x11 lattice)



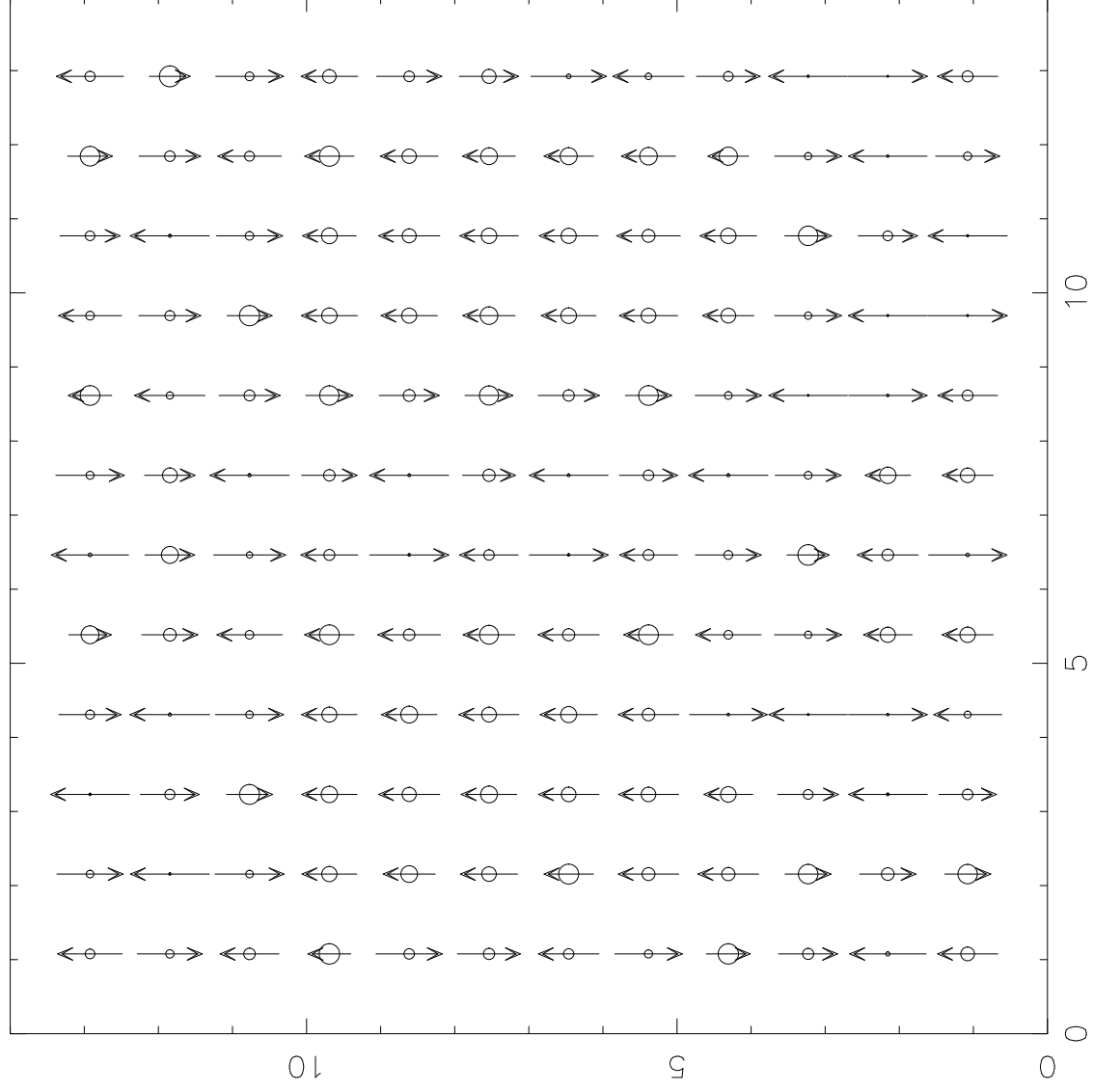
nagaoka ,  $h=49$ ,  $U=8$ ,  $t_2=0.3$



non-collinear fmSDW,  $h=24$ ,  $U=8$ ,  $t_2=0.3$

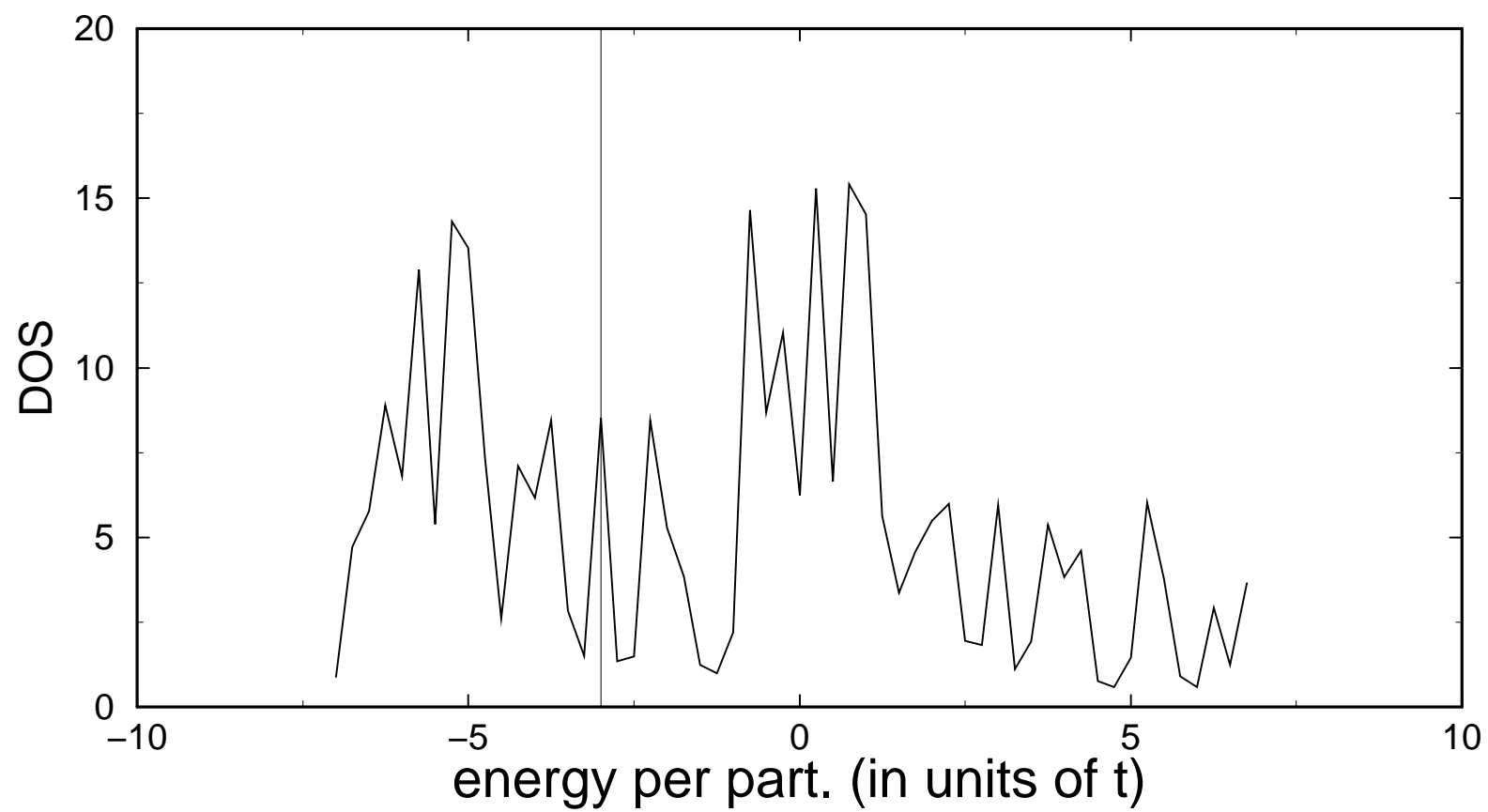


fm domains ,  $h=36$ ,  $U=8$ ,  $t_2=0.3$



# Density of states of Nagaoka FM

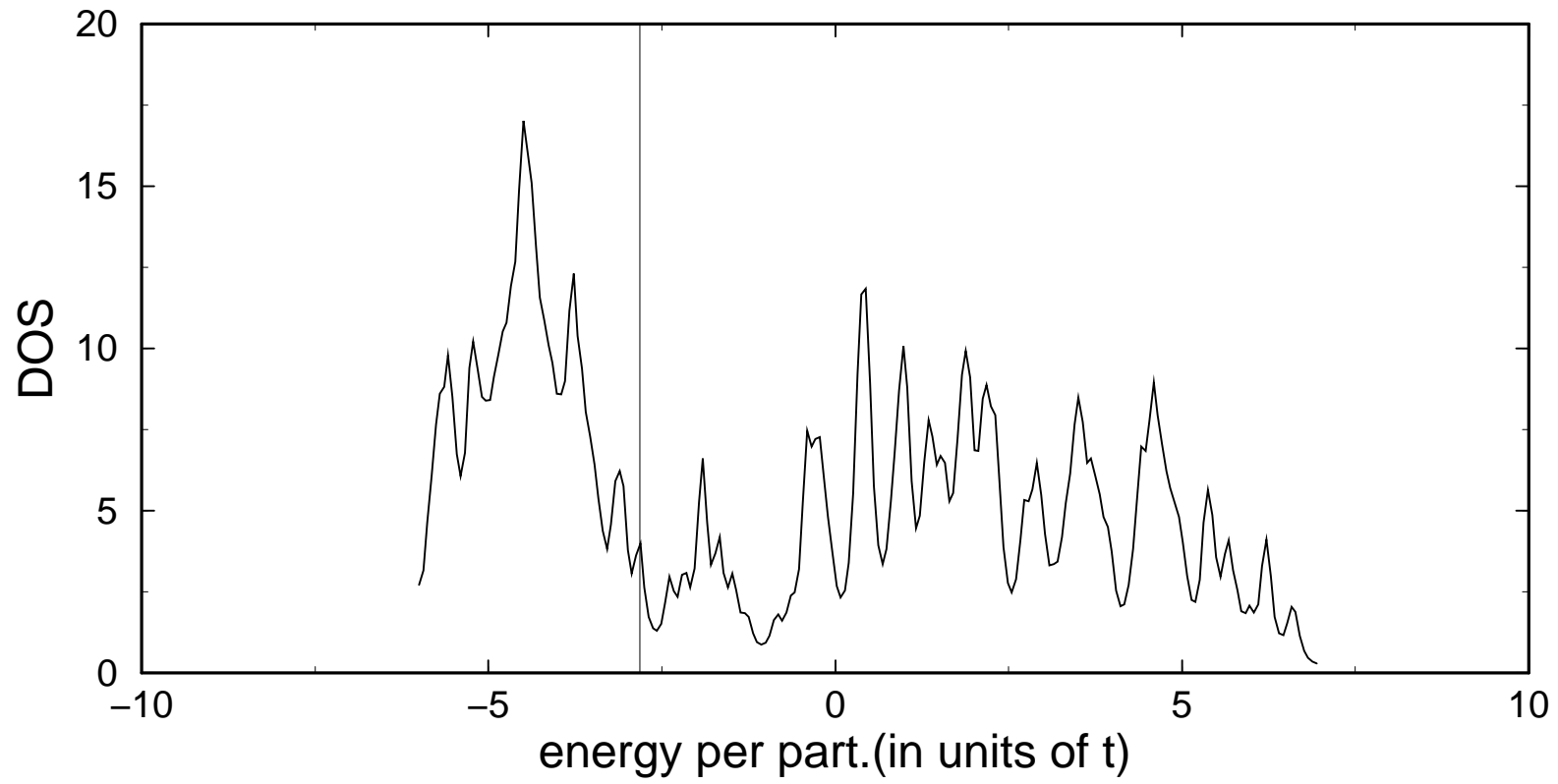
$U=8$ ,  $t'=0.3$ ,  $h=37$





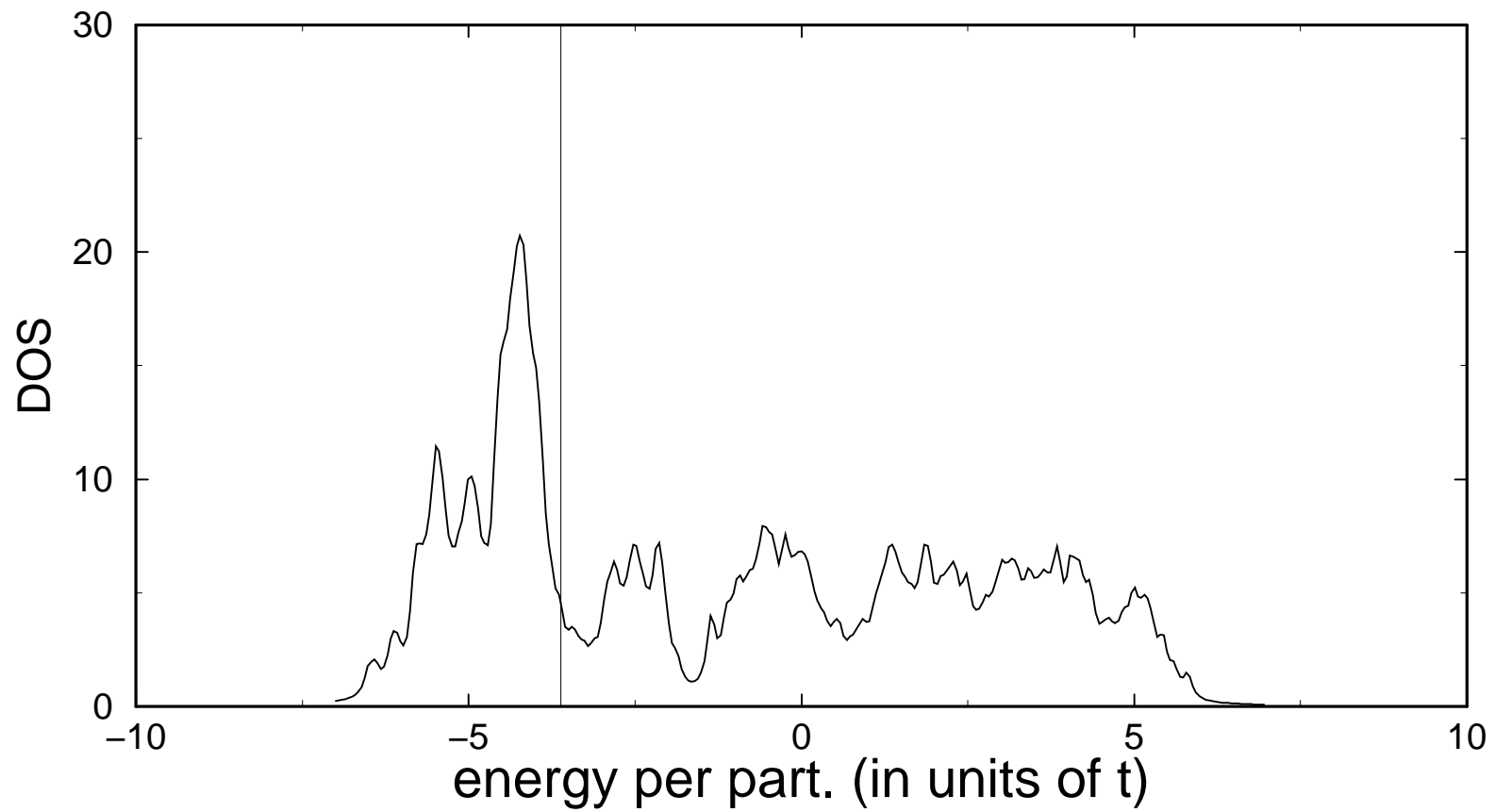
# Density of states of FM SDW

$U=8$ ,  $t'=0.3$ ,  $h=24$



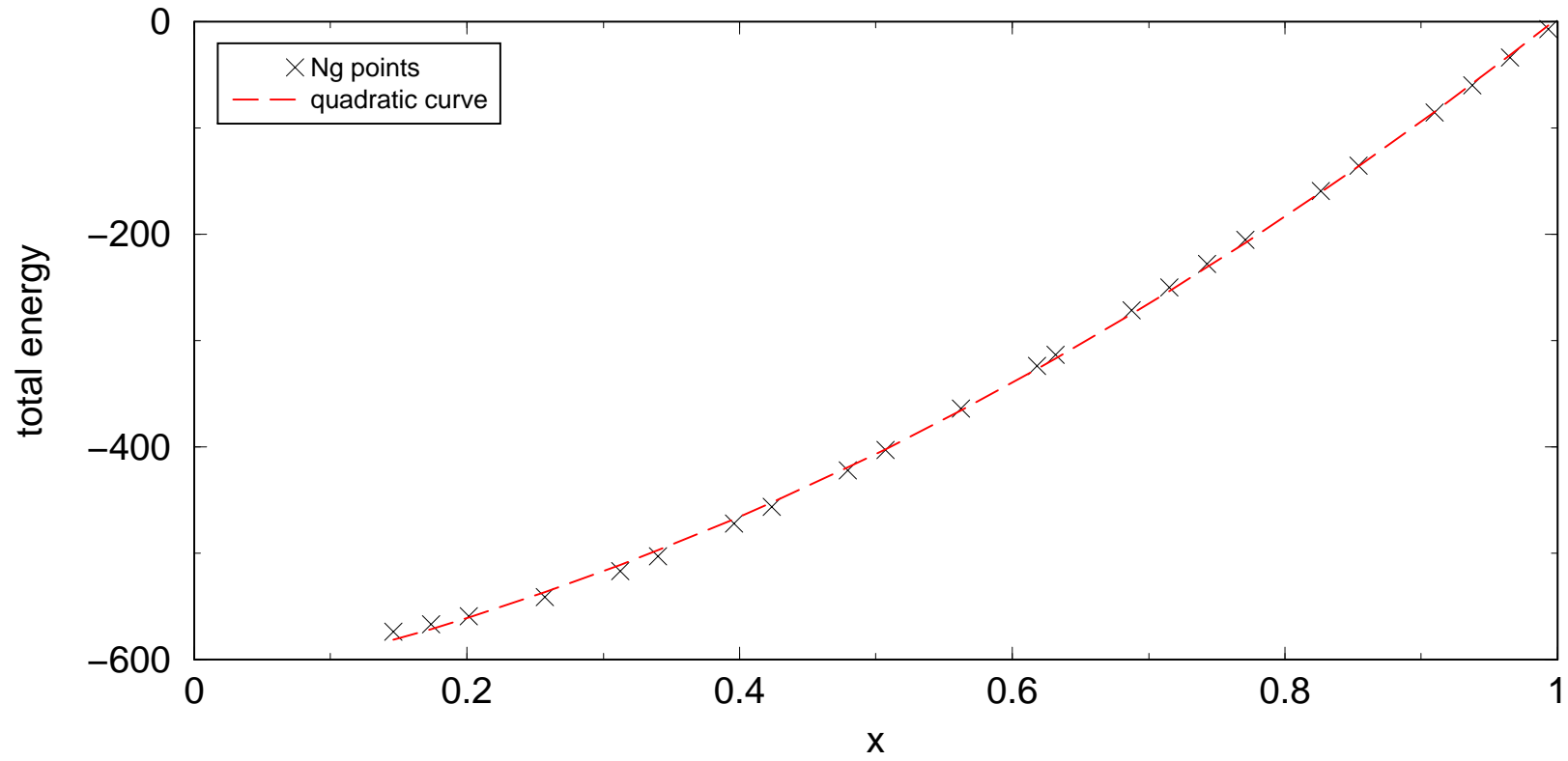
# Density of states of FM dom.

$U=8$ ,  $t'=0.3$ ,  $h=36$



# Total energy vs doping for Ng state

( $U=8$ ,  $t'=0.3$ )



# DOS of polarons

$U=8$ ,  $t'=0.3$ ,  $h=14$

